IOSR Journal of Mathematics (IOSR-JM)
e-ISSN: 2278-5728, p-ISSN: 2319-765X. Volume 17, Issue 2 Ser. I (Mar. – Apr. 2021), PP 24-38
www.iosrjournals.org

Examination of Engine oil-based ((MWCNTs-TiO_2), (MWCNTs-Al_2O_3), (MWCNTs-Cu)) Hybrid Nanofluids for Optimal Nanolubricant

John A. Okello[1], Anselm O. Oyem[2], and Winifred N. Mutuku[3]
[1&3] *(Department of Mathematics and Actuarial Science, Kenyatta University, Kenya)*
[2] *(Department of Mathematical Sciences, Federal University Lokoja, Nigeria)*

Abstract: *Oil-based lubricants with nanoparticle additives perform better in high-temperature applications compared to pure ones. High temperatures accelerate the decomposition of pure oil-based lubricants limiting their use. The use of nanoparticle enhanced lubricants (nanolubricants) is advantageous in maintaining a lower coefficient of friction, improving load-bearing capacity, and improving friction and wear resistance as opposed to pure lubricants. The current paper examines three different hybrid nanoparticle combinations* $((MWCNTs - TiO2, MWCNTs - Al2O3, MWCNTs - Cu$ *dispersed in engine oil to establish optimal (suitable) nanolubricant. The study considers steady laminar incompressible two-dimensional MHD boundary layer flow of electrically conducting engine oil based hybrid nanolubricants past a convectively heated porous vertical semi-infinite flat plate under the combined effects of buoyancy forces and Navier slip condition. The governing non-linear partial differential equations of fluid flow are transformed using suitable similarity transformation variables into a system of coupled non-linear ordinary differential equations and the numerical solution executed using the shooting technique together with the fourth-order Runge-Kutta-Fehlberg integration scheme. The numerical simulation and graphical display of results is achieved using MATLAB application. From the study, there is an increase in fluid velocity and a decrease in local skin friction with increasing values of slip parameter* (β)*, but the reverse was observed with increasing values of magnetic field intensity* (Ha)*, nanoparticle volume fraction* (ϕ)*, Eckert number* (Ec)*, Grashof number* (Gr)*, and the suction/injection parameter* (f_w)*. Both the temperature and the thermal boundary layer thickness are enhanced by increasing the magnetic field intensity* (Ha)*, nanoparticle volume fraction* (ϕ)*, and Eckert number* (Ec)*, while the cooling effect on the convectively heated plate surface is enhanced by increasing the velocity slip parameter* (β) *and suction parameter* (f_w)*. Of the three hybrid nano additives* $((MWCNTs - TiO_2), (MWCNTs - Al_2O_3), (MWCNTs - Cu))$ *considered in the study, the use of* $(MWCNTs - TiO_2)$ *hybrid nano additives in the engine oil resulted in the least coefficient of skin friction hence becoming the most suitable (optimal) lubricant additive.*

Keywords: *Hybrid nanofluids, Nanolubricants, Magnetohydrodynamic (MHD) flow.*

Date of Submission: 18-02-2021 Date of Acceptance: 03-03-2021

I. Introduction

Solid lubricants such as graphite are less volatile and are thus preferred as lubricants in high-temperature applications [1–3]. The use of petroleum-based lubricants (such as oil and grease) in high-temperature lubrication is limited due to their high volatility. Studies have shown that dispersing nanoparticles in petroleum-based lubricants enhances their use in high-temperature applications [4–6]. The nanoparticles used in the enhancement of lubricants are made of metals $(Cu, Ag, Ni, \text{and } Au)$, metal oxides$(Al_2O_3, CuO, MgO, ZnO, SiO_2, Fe_2O_3, \text{and } TiO_2)$, and metal carbide (SiC) (SiC), metal nitride (AIN), or Carbon materials (CNTs, MWCNTs, diamond, and graphite).

The use of nanoparticles as lubricant additives is achieved in two ways (use of single nanoparticles or hybrid nanoparticles). The use of Hybrid nanoparticles in the enhancement of lubricants for friction reduction is promising [7]. Several authors have studied the use of hybrid nanoparticles as lubricant additives [8–11]. Investigations by [12] on $(\text{alumina} - MoS_2)$ hybrid nanoparticle enriched cutting fluid in turning of AISI 304 stainless steel reported reduction in cutting force, feed force, thrust force, and surface roughness by $7.35\%, 18.08\%, 5.73\%, \text{and } 2.38\%$ respectively compared to Al_2O_3 mixed nanofluid. [13] investigating dynamic viscosity of $(\text{MWCNT} - TiO_2/10w40 \text{ engine oil})$ hybrid nanofluid observed an 80% reduction in viscosity of the nanofluid with rising temperature. They also noted a 100% increment in viscosity for nanofluids containing 0.75% solid volume fractions of MWCNTs. The study by [14] on the use of (MWCNT –

$ZnO/5W50 -$ engine oil) nanolubricant in lighter-duty vehicles registered a significant decrease in viscosity of nanolubricant compared to pure 5W50 oil upon dispersion of MWCNT (0.05%) and ZnO (0.1%) nanoparticles. The reduction in viscosity was significant in minimizing damage caused to the engine in cold start conditions. The assessment by [15] on tribological properties of $(ZnO/\text{engine oil})$ nanofluid in boundary lubrication reported a reduction in coefficient of friction and specific wear rate of the piston ring by $(20 - 23\%)$ and $(43 - 88\%)$ respectively in reference to oil. The reduction in both coefficients of friction and wear rate was attributed to the formation of a solid tribofilms layer on the sliding surfaces that prevented the surfaces from coming into direct contact. [16] using engine oil (SAE50) doped with Zinc oxide nanoparticles observed enhancement in viscosity of the nanolubricant with rising nanoparticle concentration. The maximum enhancement of 25.3% in viscosity in relation to the base fluid was obtained. The study further revealed a decrease in viscosity with rising temperatures. [17] evaluating the performance of CuO and (Cu/Ag) alloy as nano additives in refrigerant compressor oil observed a lower coefficient of friction in (Cu/Ag) alloy nanolubricant. The coefficient of friction in (Cu/Ag) alloy nanolubricant was 5.5% lower than that of CuO nanolubricant and 9.9% lower than that of pure lubricant. The experiment also reported enhancement in the coefficient of performance (COP) at 0.5vol% of (Cu/Ag) alloy and CuO nanolubricants to be 20.88% and 14.55% respectively compared to pure lubricant. In their study [18] on different nanoparticles materials $(SiO_2, TiO_2, \text{and } ZnO)$ suspended in the base oil, they reported a reduction in coefficient of friction (COF) and enhancement in anti-wear ability at nanoparticle concentration of $1.0\text{wt.}\%$ with (SiO_2/oil) nanolubricant registering 45.6% and 35% reduction in COF and area of wear scar respectively. [19] examining tribological properties of (CeO_2/CuO) coconut oil-based hybrid nanolubricant, they recorded 15.7% and 23.4% reduction in coefficient of friction and wear scar diameter respectively upon use of 0.25wt% $(CeO_2/CuO: 50/50)$ hybrid nanolubricant compared to pure coconut oil. The study by [20] on $(\text{MWCNT/Turbine meter oil}) -$ based nanofluid, revealed enhancement in friction coefficient for all concentrations of MWCNT in pure oil. The highest enhancement recorded was 10.41% at 0.3wt% nanoparticle concentration and 0.069m/s inlet velocity.

Apart from being used as lubricant additives (enhancers) owing to their advanced thermal conductivity, Nanofluids have also been utilized as coolant fluids in automobile radiators [21], In the biomedical field, they are used in speeding up the freezing of tumour cells (cancerous cells) through nanocryosurgery. Magnetic nanoparticles (ferrofluids) are used to deliver drugs and radiation to cancer patients. Nanoparticles have also been used as contrast agents in Magnetic Resonance Imaging (MRI) and in magnetic fluid hyperthermia to destroy cancer cells [22–25].

The purpose of the current study is to investigate two dimensional steady laminar magnetohydrodynamic boundary layer flow of electrically conducting engine oil-based hybrid nanolubricants past a convectively heated porous vertical semi-infinite flat plate under the combined effects of buoyancy forces and Navier slip condition. The equations governing the flow (non-linear partial differential equations) are transformed to a system of coupled non-linear ordinary differential equations using suitable similarity transformation variables and the numerical solution executed using the shooting technique together with the fourth-order Runge-Kutta-Fehlberg integration scheme. The numerical simulation and graphical display of results is achieved using the MATLAB application. A detailed discussion on the effect of pertinent parameters on velocity profile, temperature profile, local skin friction, and local Nusselt number of the engine oil-based hybrid nanolubricant is then given.

II. Mathematical Formulation

A steady laminar incompressible two-dimensional MHD boundary layer flow of an electrically conducting engine oil based hybrid nanolubricant past a convectively heated porous vertical semi-infinite flat plate under the combined effects of buoyancy forces and Navier slip is considered. The engine oil based hybrid nanolubricants consists of (MWCNTs/TiO_2), (MWCNTs/Al_2O_3), and (MWCNTs/Cu) hybrid nanoparticle combinations. The x-axis is taken along the direction of the plate, and the y-axis perpendicular to it. The left side of the plate is heated convectively by a hot fluid at a temperature T_f with a heat transfer coefficient h_f. The right surface of the plate is exposed to a stream of electrically conducting engine oil based cold hybrid nanolubricant at a temperature T_∞ in the presence of a transverse magnetic field of strength B_0 applied parallel to y-axis as illustrated in figure 1.

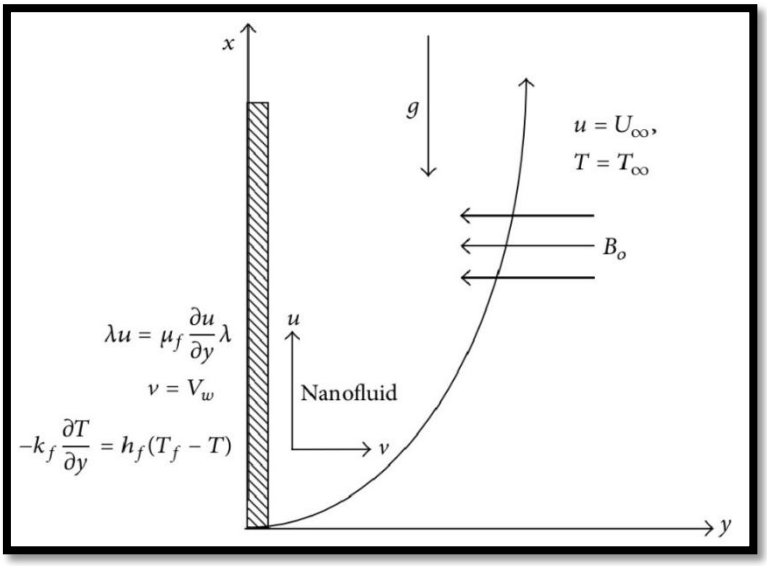

Figure.1: Flow configuration and coordinate system

The induced magnetic field due to the motion of the electrically conducting fluid is negligible. The external electrical field is assumed to be zero and the electric field due to the polarization of charges is negligible.
Assuming a Boussinesq incompressible fluid model, the equations of conservation of mass, momentum, and energy equation for the flow are given as:

$$\frac{\partial u}{\partial x} + \frac{\partial v}{\partial y} = 0 \tag{1}$$

$$u\frac{\partial u}{\partial x} + v\frac{\partial u}{\partial y} = U_\infty \frac{dU_\infty}{dx} + \frac{\mu_{hnf}}{\rho_{hnf}}\frac{\partial^2 u}{\partial y^2} + \beta_{hnf} g(T - T_\infty) - \frac{\sigma_{hnf} B_0^2 (u - U_\infty)}{\rho_{hnf}} \tag{2}$$

$$u\frac{\partial T}{\partial x} + v\frac{\partial T}{\partial y} = \frac{k_{hnf}}{(\rho C_p)_{hnf}}\frac{\partial^2 T}{\partial y^2} + \frac{\mu_{hnf}}{(\rho C_p)_{hnf}}\left(\frac{\partial u}{\partial y}\right)^2 + \frac{\sigma_{hnf} B_0^2 (u - u_\infty)^2}{(\rho C_p)_{hnf}} \tag{3}$$

Subject to the boundary conditions (BCs):

$$at\ y = 0,\ \ \lambda u = \mu_f \frac{\partial u}{\partial y}, \quad v = v_W, \quad -k_f \frac{\partial T}{\partial y} = h_f(T_f - T)$$
$$at\ \ y = \infty, \quad U = U_\infty, \quad T = T_\infty \tag{4}$$

The dimensionless variables (5) are introduced to simplify the mathematical analysis of the problem.

$$\eta = (a/v_f)^{1/2} y, \qquad \psi = (a v_f)^{1/2} x f(\eta) \qquad \theta(\eta) = \frac{T - T_\infty}{T_f - T_\infty} \tag{5}$$

Introducing the stream function $\psi(x, y)$ in the flow and defining u and v as in equation (6) the equation of continuity is satisfied automatically as in equation (7)

$$u = \frac{\partial \psi}{\partial y}, \qquad v = -\frac{\partial \psi}{\partial x} \tag{6}$$

$$\frac{\partial}{\partial x}\left(\frac{\partial \psi}{\partial y}\right) + \frac{\partial}{\partial y}\left(-\frac{\partial \psi}{\partial x}\right) = \frac{\partial^2 \psi}{\partial x \partial y} - \frac{\partial^2 \psi}{\partial x \partial y} = 0 \tag{7}$$

Using equations (5) to solve the momentum and energy equations (2) and (3) we obtain equation (8) and (9) respectively

$$f'''(\eta)+(1-\phi)^{2.5}\left(1-\phi+\frac{\phi_1\rho_1+\phi_2\rho_2}{\rho_{bf}}\right)f(\eta)f''(\eta)-(1-\phi)^{2.5}\left(1-\phi+\frac{\phi_1\rho_1+\phi_2\rho_2}{\rho_{bf}}\right)\left(f'(\eta)\right)^2+(1-\phi)^{2.5}\left(1-\phi+\frac{\phi_1\rho_1+\phi_2\rho_2}{\rho_{bf}}\right)+(1-\phi)^{2.5}\left(1-\phi+\frac{\phi_1\rho_1+\phi_2\rho_2}{\rho_{bf}}\right)\left(1-\phi+\frac{\phi_1\rho_1+\phi_2\rho_2}{\rho_{bf}}\right)Gr\theta(\eta)-(1-\phi)^{2.5}\left(1-\phi+\frac{\phi_1\rho_1+\phi_2\rho_2}{\rho_{bf}}\right)\left(1-\phi+\frac{\phi_1\sigma_1+\phi_2\sigma_2}{\sigma_{bf}}\right)Ha(f'(\eta)-1)=0 \tag{8}$$

$$\theta''(\eta)+\frac{Pr\,k_{bf}}{k_{hnf}}\left(1-\phi+\frac{\phi_1(\rho C_P)_1+\phi_2(\rho C_P)_2}{(\rho C_P)_{bf}}\right)f(\eta)\theta'(\eta)+\frac{\mathrm{Pr}\,Ec\,k_{bf}}{(1-\phi)^{2.5}k_{hnf}}\left(f''(\eta)\right)^2+Ha\,\mathrm{Pr}\,Ec\left(\frac{k_{bf}}{k_{hnf}}\right)\left(1-\phi+\frac{\phi_1\sigma_1+\phi_2\sigma_2}{\sigma_{bf}}\right)(f'(\eta)-1)^2=0 \tag{9}$$

Where;

$$\phi=\phi_1+\phi_2,\qquad \frac{\rho_{hnf}}{\rho_{bf}}=1-\phi+\frac{\phi_1\rho_1+\phi_2\rho_2}{\rho_{bf}} \tag{10a}$$

$$\frac{\beta_{hnf}}{\beta_{bf}}=1-\phi+\frac{\phi_1\beta_1+\phi_2\beta_2}{\beta_{bf}},\quad \frac{\sigma_{hnf}}{\sigma_{bf}}=1-\phi+\frac{\phi_1\sigma_1+\phi_2\sigma_2}{\sigma_{bf}} \tag{10b}$$

$$\mu_{hnf}=\mu_{bf}(1-\phi)^{-2.5}\Longrightarrow\left({}^{\mu_{bf}}/_{\mu_{hnf}}\right)=(1-\phi)^{2.5} \tag{10c}$$

Taking into account the variable plate surface permeability and the hydrodynamic slip boundary functions defined respectively as:

$$V_w=-f_w\left(av_f\right)^{1/2},\qquad \lambda u(x,0)=\mu_f\frac{\partial u}{\partial y}(x,0) \tag{11}$$

The boundary conditions are transformed to:

$$f(0)=f_w,\quad f'(0)=\beta f''(0),\qquad \theta'(0)=Bi[\theta(0)-1]$$

$$f'(\infty)=1,\quad \theta(\infty)=0 \tag{12}$$

The prime symbol denotes derivative with respect to η, f_w is a constant with $f_w>0$ representing suction rate at the plate surface, $f_w<0$ corresponds to injection, $f_w=0$ shows an impermeable surface, $\lambda=0$ represents a highly lubricated surface, and $\lambda=\infty$ denotes a normal surface. The local Reynolds number (Re_x), Grashof number (Gr), Hartmann number (Ha), Prandtl number (Pr), Eckert number (Ec), slip parameter (β), and Biot number (Bi), are defined as:

$$Re_x=\frac{U_\infty x}{\upsilon_f},\qquad Gr=\frac{\beta_{hnf}g\left(T_f-T_\infty\right)}{a^2x},\qquad Ha=\frac{\sigma_{hnf}B_0^2}{a\rho_{hnf}}$$

$$Pr=\frac{\upsilon_f}{\propto_{bf}},\qquad Ec=\frac{a^2x^2}{(C_p)_{hnf}(T_f-T_\infty)},\qquad \beta=\frac{\mu_f}{\lambda}\sqrt{\frac{a}{\upsilon_f}},\qquad Bi=\frac{h_f}{k_f}\sqrt{\frac{\upsilon_f}{a}} \tag{13}$$

The physical quantities of practical significance in this work are the skin friction coefficient C_f and the local Nusselt number Nu, which are expressed as

$$C_f=\frac{\tau_w}{\rho_f U_\infty^2},\qquad Nu=\frac{xq_w}{k_f\left(T_f-T_\infty\right)} \tag{14}$$

Where τ_w is the skin friction and q_w is the heat flux from the plate which are given by

$$\tau_w=\mu_{hnf}\left.\frac{\partial u}{\partial y}\right|_{y=0},\qquad q_w=-k_{hnf}\left.\frac{\partial T}{\partial y}\right|_{y=0} \tag{15}$$

Substituting (15) into (14)

$$Re_x^{1/2} C_f = \frac{\mu_{hnf}}{\upsilon_f \rho_f \beta} f'(0) = \frac{\mu_{hnf}}{\upsilon_f \rho_f} f''(0) = \frac{1}{(1-\phi_1)^{2.5}(1-\phi_2)^{2.5}} f''(0) \quad (16a)$$

$$Re_x^{-\frac{1}{2}} Nu = -\frac{k_{hnf}}{k_f} \theta'(0) \quad (16b)$$

The set of equations $(8-9)$ together with the boundary conditions (12) are solved using the shooting technique coupled with the fourth-order Runge-Kutta-Fehlberg iteration scheme.
Defining the new variables as

$$x_1 = f, \qquad x_2 = f', \qquad x_3 = f'', \qquad x_4 = \theta, \qquad x_5 = \theta' \quad (17)$$

The equations $(8-10)$ are transformed into a set of initial value problems (a system of first-order differential equations) $(18-19)$ with initial values conditions (21) below

$$x_3' = -A_1[x_1 x_3 - x_2^2 + 1 + A_2 Gr x_4 - A_3 Ha(x_2 - 1)] \quad (18)$$

$$x_5' = -\frac{Pr k_{bf}}{k_{hnf}} \left(A_4 x_1' x_5 + \frac{Ec}{(1-\phi)^{2.5}} x_3^2 + Ha\, Ec\, A_3 (x_2 - 1)^2 \right) \quad (19)$$

Where

$$A_1 = (1-\phi)^{2.5} \left(1 - \phi + \frac{\phi_1 \rho_1 + \phi_2 \rho_2}{\rho_{bf}} \right), \qquad \phi = \phi_1 + \phi_2 \quad (20a)$$

$$A_2 = 1 - \phi + \frac{\phi_1 \beta_1 + \phi_2 \beta_2}{\beta_{bf}} \quad (20b)$$

$$A_3 = 1 - \phi + \frac{\phi_1 \sigma_1 + \phi_2 \sigma_2}{\sigma_{bf}} \quad (20c)$$

$$A_4 = 1 - \phi + \frac{\phi_1 (\rho C_P)_1 + \phi_2 (\rho C_P)_2}{(\rho C_P)_{bf}} \quad (20d)$$

$$k_{hnf} = \frac{2(1-\phi) k_{bf} + (1+2\phi_1) k_1 + (1+2\phi_2) k_2}{(2+\phi) k_{bf} + (1-\phi_1) k_1 + (1-\phi_2) k_2} \quad (20e)$$

The equations (18) and (19) are subject to the initial conditions (21) below

$$x_1(0) = f_w, \quad x_2(0) = \beta x_3(0), \quad x_5(0) = Bi[x_4(0) - 1]$$

$$x_2(\infty) = 1 \qquad x_4(\infty) = 0 \quad (21)$$

From the process of numerical computation, the fluid velocity, the temperature, the skin friction coefficient, and the Nusselt number are proportional to $f'(\eta), \theta(\eta), f''(\eta)$, and $\theta'(\eta)$, respectively.

III. Results and Discussion

The physical parameters involved in the flow are numerically computed to ascertain their effect on fluids velocity profile, temperature profile, skin friction coefficient, and Nusselt number, and the graphical display of the result is provided in figures $(2-21)$. These parameters are the magnetic field intensity (Ha), Prandtl number (Pr), slip parameter (β), Eckert number (Ec), nanoparticle volume fraction (ϕ), and suction/injection parameter (f_w). The three-engine oil-based hybrid nanolubricant considered in the study are $\left((MWCNTs - Cu/engine\ oil), (MWCNTs - Al_2O_3/engine\ oil), and\ (MWCNTs - TiO_2/engine\ oil) \right)$ hybrid nanolubricants. Table 1 gives the thermophysical properties of both the engine oil and the nanoparticles used in the study.

Table.1: Thermophysical properties of Engine oil and nanoparticles [26-27]

Materials	$\rho(kg/m^3)$	$C_P(J/kgK)$	$k(W/mK)$	$\beta(K^{-1})$	$\sigma(S/m)$
Engine oil	804	1909	0.145	70×10^{-5}	1×10^{-7}
MWCNTs	1600	796	3000	1.6×10^{-5}	1×10^{5}
Alumina (Al_2O_3)	3970	765	40	0.85×10^{-5}	35×10^{6}
Titania (TiO_2)	4250	686.2	8.9538	0.9×10^{-5}	1×10^{-12}
Copper (Cu)	8933	385	401	1.67×10^{-5}	5.96×10^{7}

Effect of Parameter variation on the velocity profile

Figures $(3-8)$ is the graphical display of how different parameters affects the velocity profile of the hybrid nanofluid. The hybrid nanofluids velocity on the wall of the plate is zero (the no-slip condition) and its value rises gradually to a free stream value far away from the plate satisfying the given free stream boundary conditions. Among the three engine oil-based hybrid nanofluids $((MWCNTs-Cu), (MWCNTs-Al2O3, \text{ and } MWCNTs-TiO2,$ the least momentum boundary layer thickness was registered in MWCNTs−Cu/engine oil hybrid nanofluid as depicted in figure *2* The closer proximity of *MWCNTs−Cu/engine oil* hybrid nanofluid to the wall of the convectively heated plate as it flows makes it a better coolant than the rest of the nanofluids. The velocity of the nanofluid also overshoots towards the wall of the plate resulting in a decrease in both the fluid's velocity and momentum boundary thickness with increasing values of Eckert number (Ec), suction/injection parameter (f_w), Grashof number (Gr), magnetic field intensity (Ha) and nanoparticle volume fraction (ϕ) as illustrated in figures $(3-7)$. The magnetic field applied perpendicular to the flow of a conductive fluid creates Lorentz force (retarding force) that slows down the moving fluid. This Lorentz force is enhanced as values of applied magnetic field intensity (Ha) increases. The ability to retard the flow of a conductive fluid by applying a magnetic field perpendicular to it has applications in MHD power generation and electromagnetic coating of wires and metal. The enhancement in fluids velocity at the wall of the plate is also triggered with increasing values of slip parameter (β) as seen in figure 8. This is in agreement with the fact that higher β implies an increase in the lubrication and slipperiness of the surface.

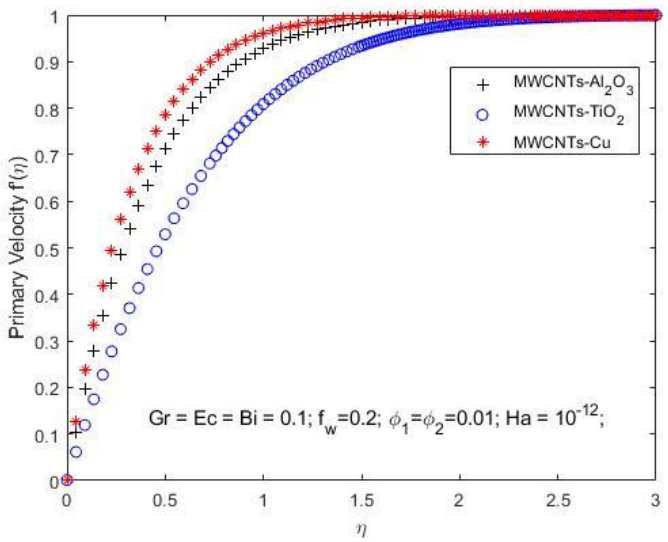

Figure.2: Velocity profile for different engine oil-based hybrid nanolubricants

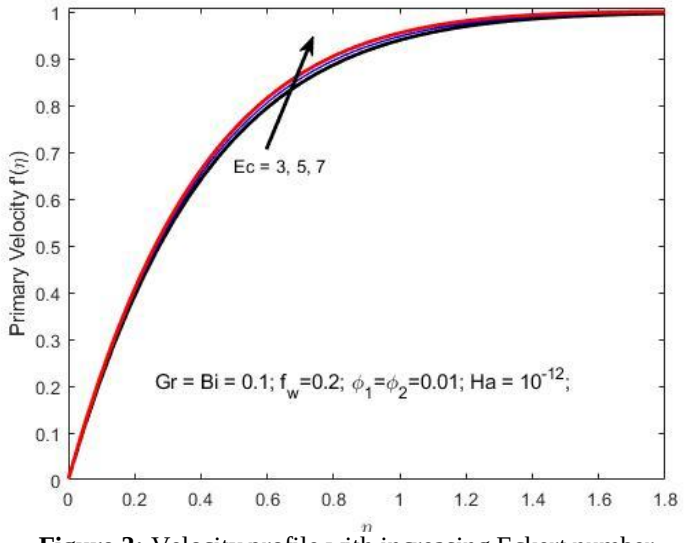

Figure.3: Velocity profile with increasing Eckert number

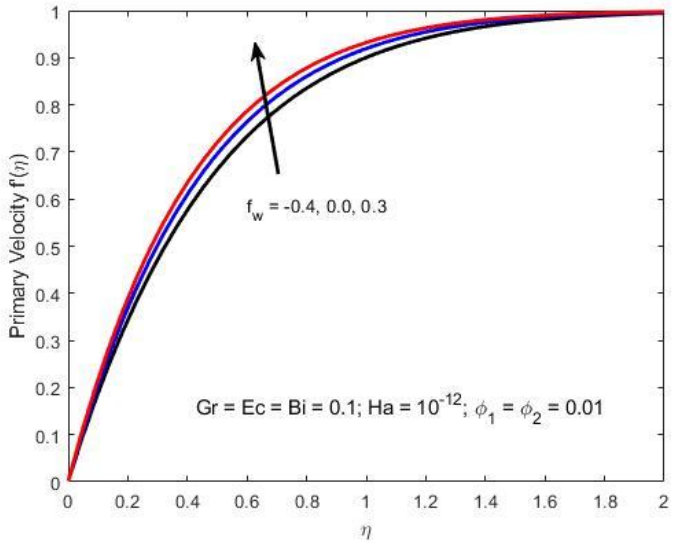

Figure.4: Velocity profile with increasing suction/injection parameter

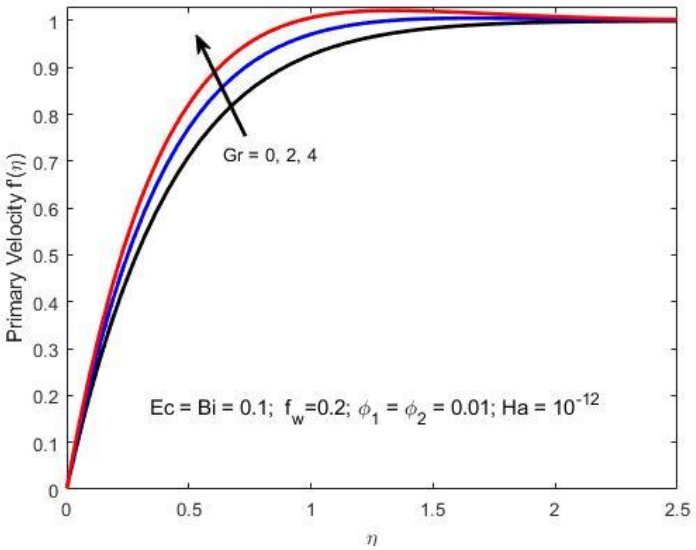

Figure.5: Velocity profile with increasing Grashof number

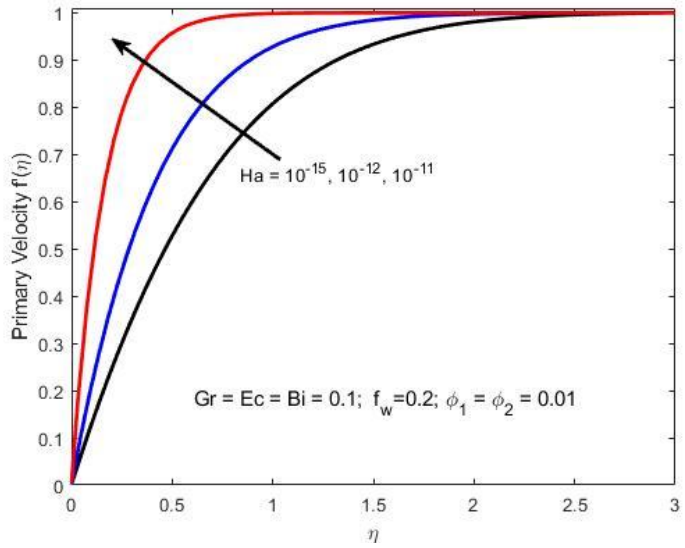

Figure.6: Velocity profile with increasing magnetic field intensity

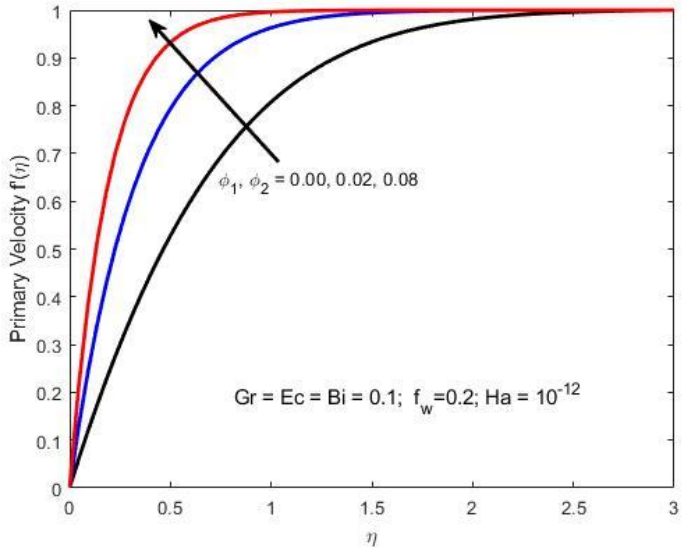

Figure.7: Velocity profile with increasing nanoparticle volume fraction

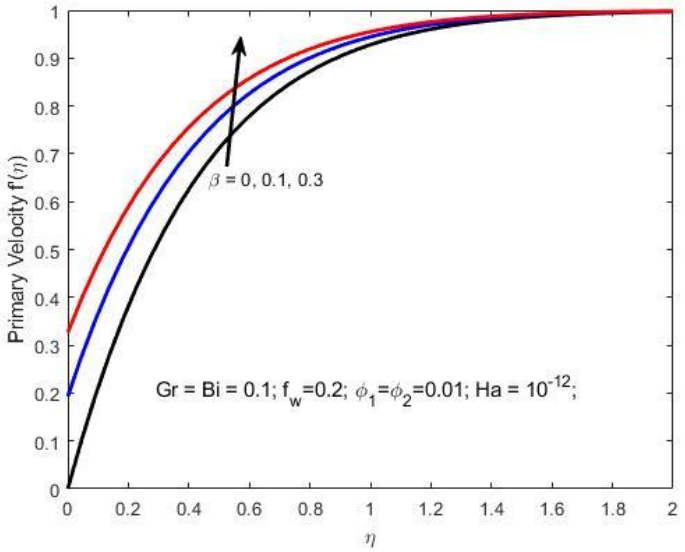

Figure.8: Velocity profiles with increasing slip parameter

Effect of Parameter variation on the temperature profile

Figures $(10-15)$ shows how different parameters influence the temperature profile of the hybrid nanolubricant. From the figures, the maximum fluid temperature occurs on the wall of the plate and this is attributed to convectional heating occurring at the surface of the plate. This maximum wall temperature decays exponentially to zero value far away from the surface of the plate to satisfy the given free stream boundary conditions. Among the three hybrid nanolubricants $(MWCNTs-Cu/engine\ oil)$ hybrid nanolubricant registered the highest wall temperature and higher thermal boundary layer thickness as depicted in figure 9. The $(MWCNTs-Cu/engine\ oil)$ hybrid nanolubricant flows closer to the surface of the plate than the rest of hybrid nanolubricants and hence tend to absorb more heat compared to the rest of the nanolubricants. The increment in fluid temperature and thermal boundary layer thickness is also observed with increasing values of magnetic field intensity (Ha), nanoparticle volume fraction (ϕ), and Eckert number(Ec) as seen in figures $(10-12)$ which is as a result of additional heating arising from increased friction between the layers of the fluid due to the presence of (Ha) and enhanced heat transfer rate to the plate from the hot fluid due to the presence of nanoparticles and additional heating due to viscous dissipation.

From the figures $(13-15)$ increment in $(Gr, f_w, and\ \beta)$ leads to a reduction in both the fluid temperature and thermal boundary layer thickness. Increase in (β) implies enhanced surface slipperiness that reduces friction and associated heat between the surface and the fluid

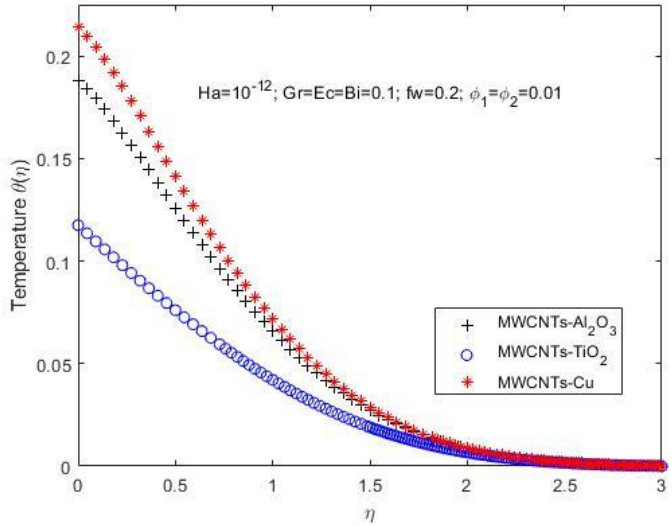

Figure.9: Temperature profile for different hybrid nanolubricants

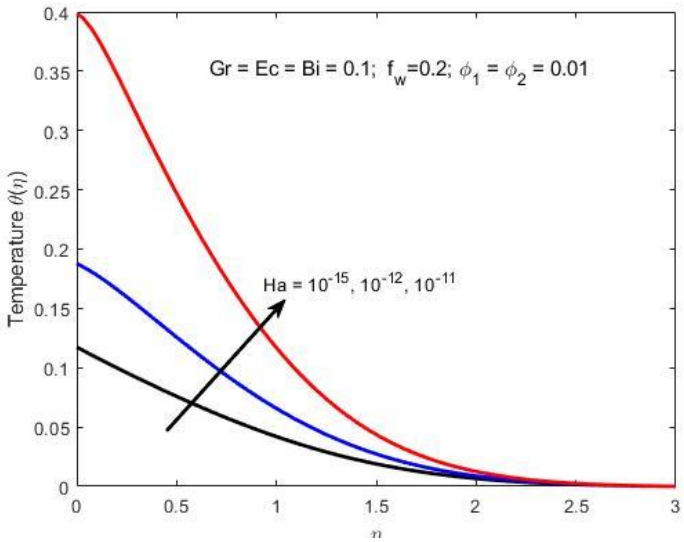

Figure.10: Temperature profile with increasing magnetic field intensity

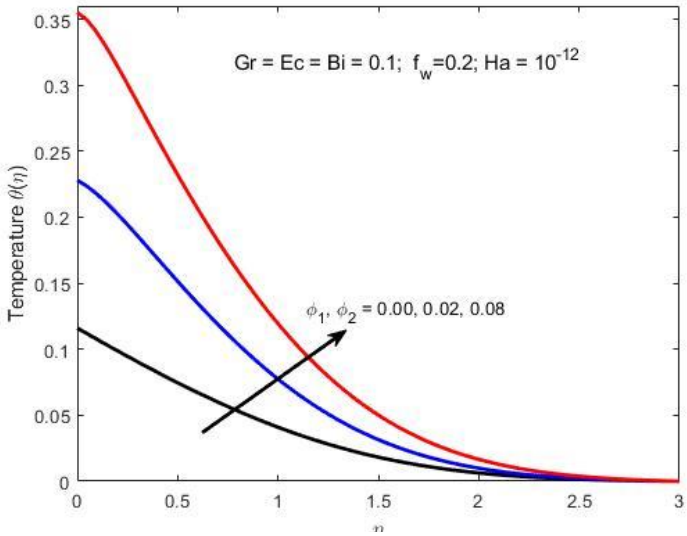

Figure.11: Temperature profile with increasing nanoparticle volume fraction

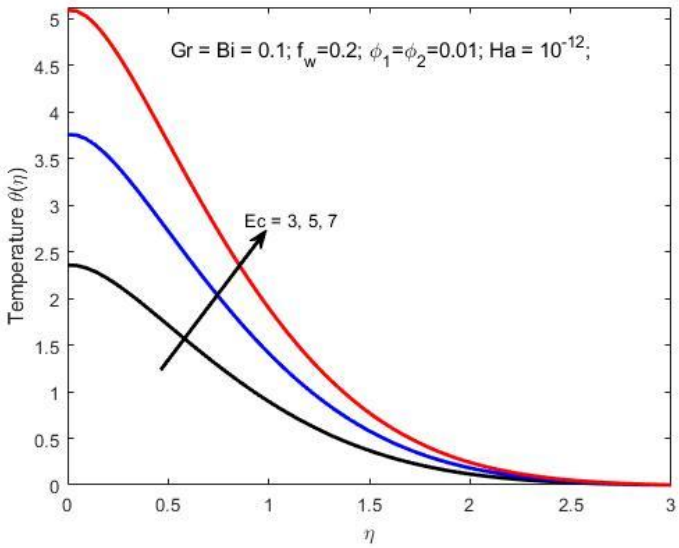

Figure.12: Temperature profile with increasing Eckert number

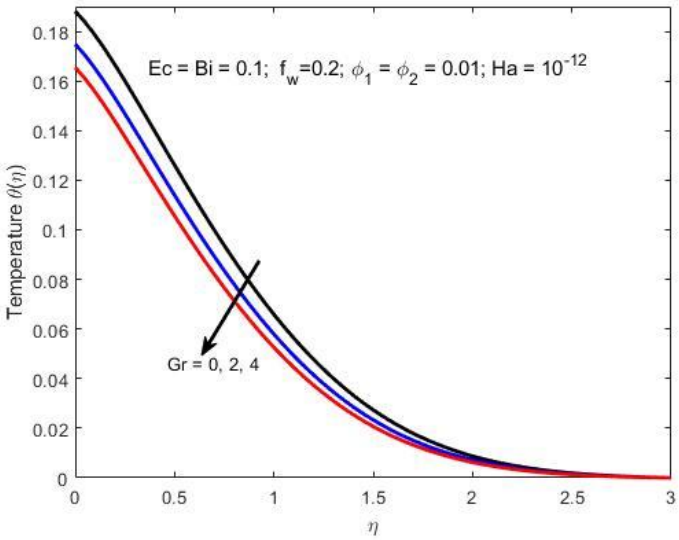

Figure.13: Temperature profile with increasing Grashof number

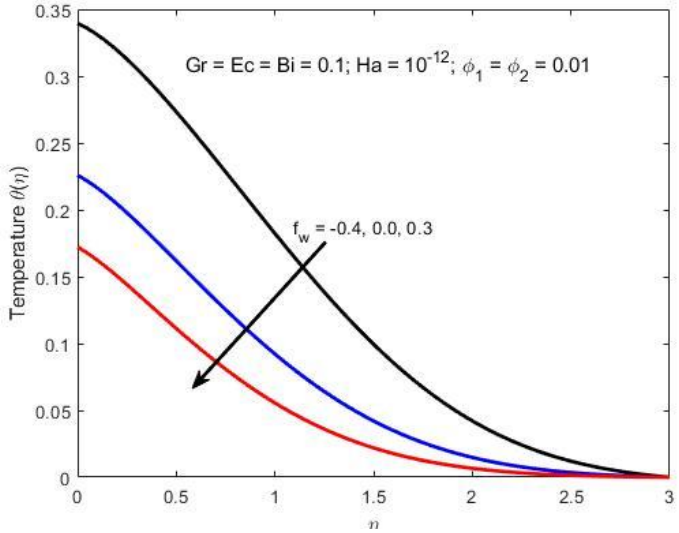

Figure.14: Temperature profile with increasing suction/injection parameter

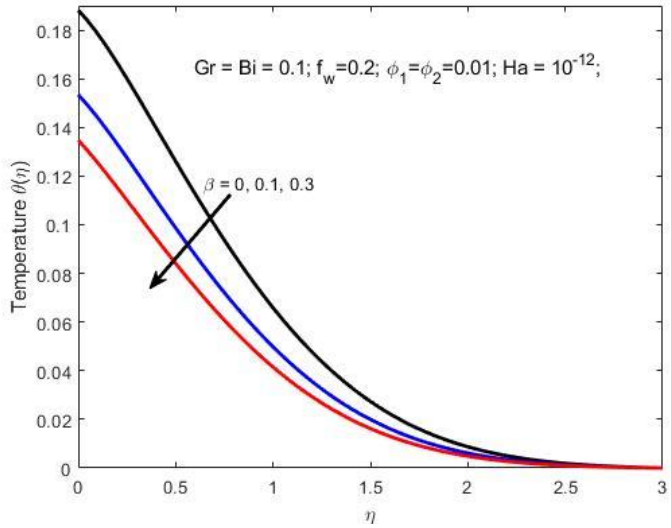

Figure.15: Temperature profile with increasing slip parameter

Effect of Parameters Variation on the Skin Friction and Nusselt Number

Figures $(16-21)$ shows how different parameters affect local skin friction coefficient and local Nusselt number (heat transfer rate) at the wall (surface of the plate). Nanoparticles suspended in normal (conventional) heat transfer fluid enhances its coefficient of friction as depicted in figure 17. For the engine oil-based hybrid nanolubricants $(MWCNTs-Cu,\ MWCNTs-Al_2O_3, and\ MWCNTs-TiO_2)$ in figure (17) increase in the volume of nanoparticles suspended (ϕ) results in an enhanced coefficient of skin friction. The $(MWCNTs-Cu/engine\ oil)$ hybrid nanolubricant shows the highest increase in the coefficient of skin friction with increasing values of (ϕ) with this being attributed to the closer proximity of $(MWCNTs-Cu/engine\ oil$ nanolubricant to the plate's surface resulting in elevation of velocity gradient on the wall of the plate. From the figures $(16\ and\ 19)$ increase in suction/injection parameter (f_w) and Grashof number (Gr) enhances the coefficient of skin friction. Higher values of slip parameter (β) implies the surface is becoming more slippery (more lubricated) resulting in a decrease in coefficient of skin friction as seen in figure 16. Increasing values of suction/injection parameter (f_w), volume of nanoparticle suspended (ϕ), and Grashof number (Gr) enhances heat transfer rate (local Nusselt number) as depicted in figures $(18,20,and\ 21)$. The $((MWCNTs-TiO_2)/engine\ oil)$ hybrid nanolubricant shows the highest increase in local Nusselt number as seen in figure 20

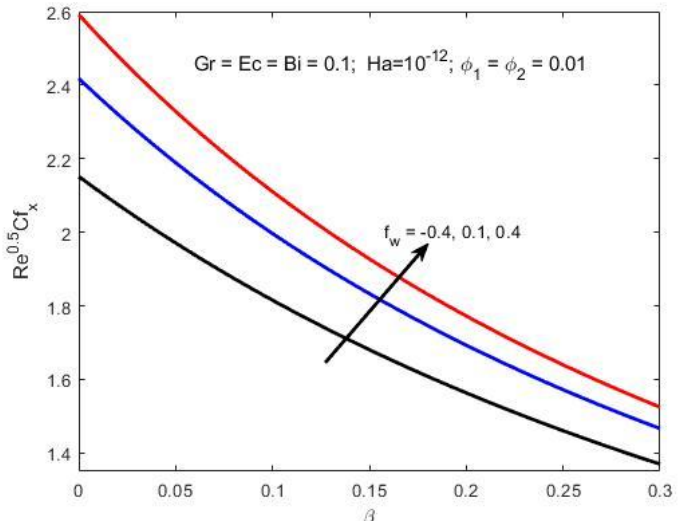

Figure.16: Effects of increasing $\boldsymbol{\beta}$ and $\boldsymbol{f_w}$ on local skin friction

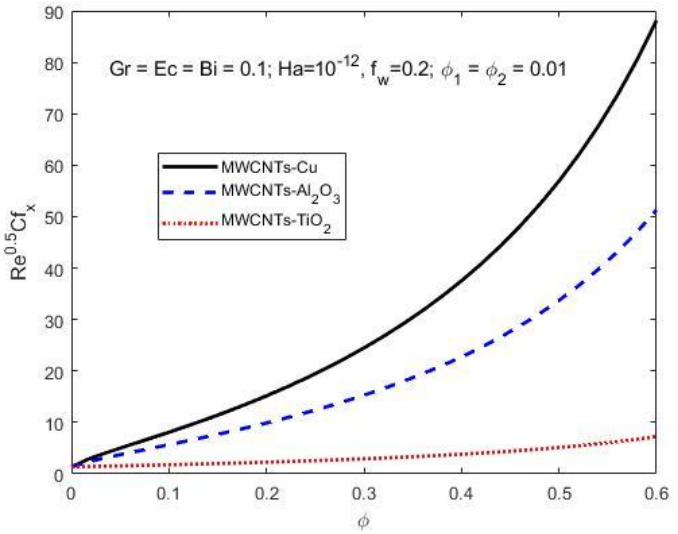

Figure.17: Local skin friction profiles for different hybrid nanolubricants

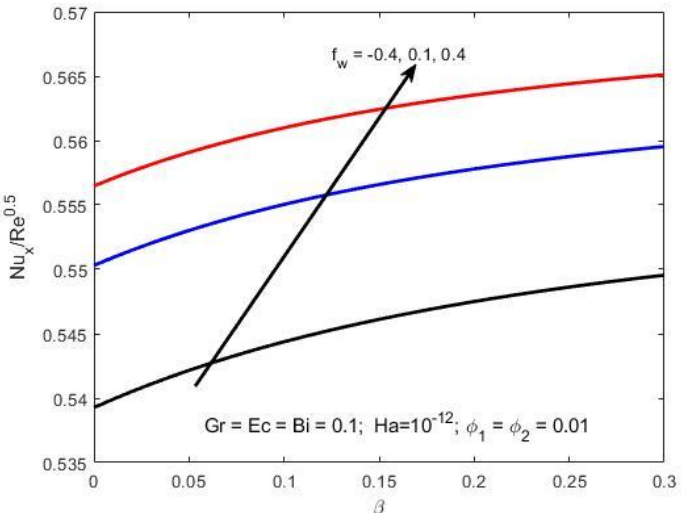

Figure.18: Local Nusselt number with increasing suction/injection parameter

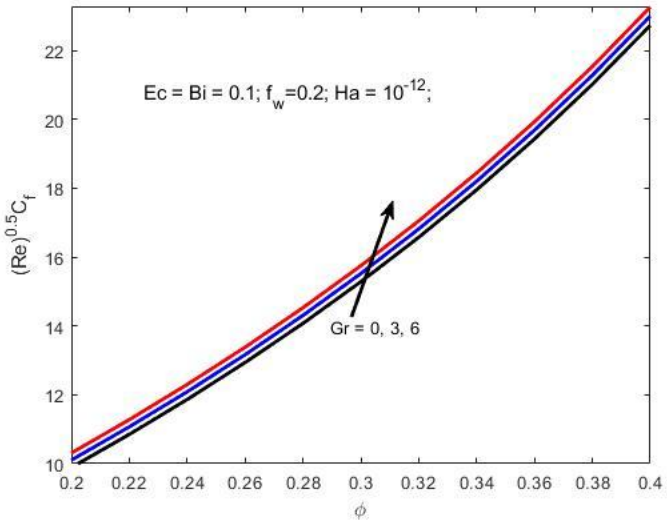

Figure.19: Local skin friction with increasing Grashof number

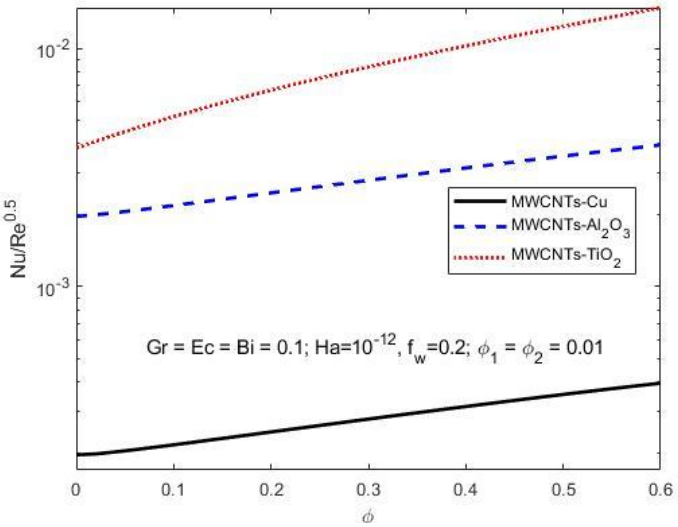

Figure.20: Local Nusselt number for different hybrid nanolubricants

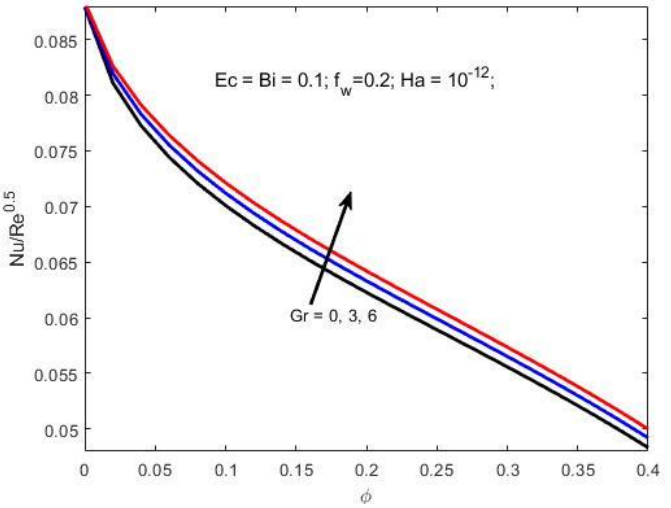

Figure.21: Effect of increasing nanoparticle volume fraction and Grashof number on Local Nusselt number

IV. Conclusion

In the study, a two-dimensional steady laminar incompressible MHD boundary layer flow of an electrically conducting engine oil based hybrid nanolubricant past a convectively heated porous vertical semi-infinite flat plate under the combined effects of buoyancy forces and Navier slip condition was considered. The hybrid nanoparticle combination used in the study were $\left((MWCNTs/TiO_2), (MWCNTs/Al_2O_3), and\ (MWCNTs/Cu)\right)$. The governing non-linear partial differential equations of fluid flow were transformed using suitable similarity transformation variables into a system of coupled non-linear ordinary differential equations and the numerical solution was executed using the shooting technique together with the fourth-order Runge-Kutta-Fehlberg integration scheme. The numerical simulation and graphical display of results were achieved using the MATLAB application. From the study the following conclusions are drawn: The fluid's velocity increases with increasing values of the slip parameter β, but decreases with increasing values of magnetic field intensity (Ha), nanoparticle volume fraction (ϕ), Eckert number (Ec), Grashof number (Gr), and the suction/injection parameter (f_w). The local skin friction decreases with increasing values of the slip parameter (β). The fluid's temperature and thermal boundary layer thickness are enhanced by increasing magnetic field intensity (Ha), nanoparticle volume fraction (ϕ), and Eckert number (Ec). The cooling effect on the convectively heated plate surface is enhanced by increasing the velocity slip parameter (β) and suction parameter (f_w).

References

[1] A. J. S. Egea, V. Martynenko, G. Abate, N. Deferrari, D. M. Krahmer, and L. N. L. de Lacalle, "Friction capabilities of graphite-based lubricants at room and over 1400 K temperatures," *Int. J. Adv. Manuf. Technol.*, vol. 102, no. 5, pp. 1623–1633, 2019.

[2] H. Han, Z. Qian, F. Meng, and Z. Cui, "Tribological performances of graphite–MoS2 coating at various high temperatures:," *Proc. Inst. Mech. Eng. Part J J. Eng. Tribol.*, vol. 233, no. 12, pp. 1888–1902, 2019.

[3] J. R. Lince, "Effective Application of Solid Lubricants in Spacecraft Mechanisms," *Lubricants*, vol. 8, no. 7, p. 74, 2020.

[4] A. Mohamed, S. Ali, T. A. Osman, and B. M. Kamel, "Development and manufacturing an automated lubrication machine test for nano grease," *J. Mater. Res. Technol.*, vol. 9, no. 2, pp. 2054–2062, 2020.

[5] M. K. A. Ali, X. Hou, and M. A. A. Abdelkareem, "Anti-wear properties evaluation of frictional sliding interfaces in automobile engines lubricated by copper/graphene nanolubricants," *Friction*, vol. 8, no. 5, pp. 905–916, 2019.

[6] J. M. L. del Río *et al.*, "Tribological Behavior of Nanolubricants Based on Coated Magnetic Nanoparticles and Trimethylolpropane Trioleate Base Oil," *Nanomaterials*, vol. 10, no. 4, p. 683, 2020.

[7] D. Kim and L. A. Archer, "Nanoscale organic-inorganic hybrid lubricants," *Langmuir*, vol. 27, no. 6, pp. 3083–3094, 2011.

[8] A. K. Sharma, J. K. Katiyar, S. Bhaumik, and S. Roy, "Influence of alumina/MWCNT hybrid nanoparticle additives on tribological properties of lubricants in turning operations," *Friction*, vol. 7, no. 2, pp. 153–168, 2018.

[9] M. K. Ahmed Ali, H. Xianjun, F. A. Essa, M. A. A. Abdelkareem, A. Elagouz, and S. W. Sharshir, "Friction and Wear Reduction Mechanisms of the Reciprocating Contact Interfaces Using Nanolubricant Under Different Loads and Speeds," *J. Tribol.*, vol. 140, no. 5, p. 051606, 2018.

[10] M. Kumar Gupta *et al.*, "Performance Evaluation of Vegetable Oil-Based Nano-Cutting Fluids in Environmentally Friendly Machining of Inconel-800 Alloy," *Materials (Basel).*, vol. 12, no. 17, p. 2792, 2019.

[11] E. Omrani, P. L. Menezes, and P. K. Rohatgi, "Effect of Micro-and Nano-Sized Carbonous Solid Lubricants as Oil Additives in Nanofluid on Tribological Properties," *Lubricants*, vol. 7, no. 25, p. 7030025, 2019.

[12] A. K. Sharma, R. K. Singh, A. R. Dixit, and A. K. Tiwari, "Novel uses of alumina-MoS2 hybrid nanoparticle enriched cutting fluid in hard turning of AISI 304 steel," *J. Manuf. Process.*, vol. 30, pp. 467–482, 2017.

[13] M. Hemmat Esfe, A. A. Abbasian Arani, M. R. Madadi, and A. Alirezaie, "A study on rheological characteristics of hybrid nano-lubricants containing MWCNT-TiO2 nanoparticles," *J. Mol. Liq.*, vol. 260, pp. 229–236, 2018.

[14] M. Hemmat Esfe, A. A. Abbasian Arani, and S. Esfandeh, "Improving engine oil lubrication in light-duty vehicles by using of dispersing MWCNT and ZnO nanoparticles in 5W50 as viscosity index improvers (VII)," *Appl. Therm. Eng.*, vol. 143, pp. 493–506, 2018.

[15] A. Elagouz, M. K. A. Ali, H. Xianjun, M. A. A. Abdelkareem, and M. A. Hassan, "Frictional performance evaluation of sliding surfaces lubricated by zinc-oxide nano-additives," *Surf. Eng.*, vol. 36, no. 2, pp. 144–157, 2019.

[16] J. Ma, A. Shahsavar, A. A. A. A. Al-Rashed, A. Karimipour, H. Yarmand, and S. Rostami, "Viscosity, cloud point, freezing point and flash point of zinc oxide/SAE50 nanolubricant," *J. Mol. Liq.*, vol. 298, p. 112045, 2020.

[17] A. C. Yilmaz, "Performance evaluation of a refrigeration system using nanolubricant," *Appl. Nanosci.*, vol. 10, no. 5, pp. 1667–1678, 2020.

[18] L. Hao *et al.*, "Tribological evaluation and lubrication mechanisms of nanoparticles enhanced lubricants in cold rolling," *Mech. Ind.*, vol. 21, no. 1, p. 108, 2020.

[19] A. Sajeeb and P. K. Rajendrakumar, "Tribological assessment of vegetable oil based CeO2/CuO hybrid nano-lubricant:," *Proc. Inst. Mech. Eng. Part J J. Eng. Tribol.*, vol. 234, no. 12, p. 135065011989920, 2020.

[20] H. Pourpasha, S. Z. Heris, O. Mahian, and S. Wongwises, "The effect of multi-wall carbon nanotubes/turbine meter oil nanofluid concentration on the thermophysical properties of lubricants," *Powder Technol.*, vol. 367, pp. 133–142, 2020.

[21] J. A. Okello, W. N. Mutuku, and A. O. Oyem, "Analysis of Ethylene Glycol (EG)-based ((Cu-Al2O3), (Cu-TiO2), (TiO2-Al2O3)) Hybrid Nanofluids for Optimal Car Radiator Coolant," *J. Eng. Res. Reports*, vol. 17, no. 2, pp. 34–50, 2020.

[22] J. A. Okello, W. N. Mutuku, and A. O. Oyem, "A Review of Nanofluids Synthesis, Factors Influencing Their Thermophysical Properties and Applications," *J. Eng. Res. Reports*, vol. 17, no. 4, pp. 1–17, 2020.

[23] E. Forte *et al.*, "Radiolabeled PET/MRI Nanoparticles for Tumor Imaging," *J. Clin. Med.*, vol. 9, no. 1, p. 89, 2019.

[24] P. Chandrasekharan *et al.*, "Using magnetic particle imaging systems to localize and guide magnetic hyperthermia treatment: tracers, hardware, and future medical applications," *Theranostics*, vol. 10, no. 7, pp. 2965–2981, 2020.

[25] S. R. Patade, D. D. Andhare, S. B. Somvanshi, S. A. Jadhav, M. V. Khedkar, and K. M. Jadhav, "Self-heating evaluation of superparamagnetic MnFe2O4 nanoparticles for magnetic fluid hyperthermia application towards cancer treatment," *Ceram. Int.*, vol. 46, no. 16, Part A, pp. 25576–25583, 2020.

[26] S. E. Ahmed, A. K. Hussein, M. A. Mansour, Z. A. Raizah, and X. Zhang, "Mhd Mixed Convection in Trapezoidal Enclosures Filled With Micropolar Nanofluids," *Nanosci. Technol. An Int. J.*, vol. 9, no. 4, pp. 343–372, 2018.
[27] N. S. bte A. Hamzah, R. Kandasamy, and R. Muhammad, "Thermal radiation energy on squeezed MHD flow of Cu, Al2O3 and CNTs-nanofluid over a sensor surface," *Alexandria Eng. J.*, vol. 55, no. 3, pp. 2405–2421, 2016.

John A. Okello, et. al. "Examination of Engine oil-based ((MWCNTs-TiO2), (MWCNTs-Al2O3), (MWCNTs-Cu)) Hybrid Nanofluids for Optimal Nanolubricant." *IOSR Journal of Mathematics (IOSR-JM)*, 17(2), (2021): pp. 24-38.